European Radiology (2019) 29:5253–5263
https://doi.org/10.1007/s00330-019-06173-0

COMPUTED TOMOGRAPHY

Is dual-phase C-arm CBCT sufficiently accurate for the diagnosis of colorectal cancer liver metastasis during liver intra-arterial treatment?

Olivier Pellerin[1,2,3] · Helena Pereira[4,5] · Claire Van Ngoc Ty[2] · Nadia Moussa[2,3] · Costantino Del Giudice[1,2,3] · Simon Pernot[2,6] · Carole Déan[3] · Gilles Chatellier[2,4,5] · Marc Sapoval[1,2,3]

Received: 11 June 2018 / Revised: 5 March 2019 / Accepted: 15 March 2019 / Published online: 1 April 2019

Abstract

Purpose This study aimed to estimate the accuracy of dual-phase C-arm cone beam computed tomography (CBCT) for the detection of colorectal cancer liver metastases, as compared with multidetector computed tomography (MDCT).

Materials and methods Between March 2014 and December 2016, 49 consecutive patients referred for intra-arterial treatment for colorectal cancer liver metastases were enrolled in a single-center observational study. All patients were examined with MDCT and with dual-phase C-arm cone beam computed tomography performed after iodine injection in the proper hepatic artery before intra-arterial treatment. Two blinded observers independently reviewed all examinations. Diagnostic accuracy was determined using both a six-cell matrix method and a "worst-case scenario."

Results Readers identified at MDCT 264 colorectal liver metastases and 43 other liver lesions. The early and late arterial phase showed 240 and 277 liver lesions respectively. A certainty of the diagnosis was obtained in 63% and 85% at the early (EAP) and late arterial phase (LAP), respectively. Streak artifacts or liver segment truncation, or inadequate enhancement was responsible for the inability to see or to correctly adjudicate a lesion to a diagnosis in 27% and 15% of the cases at the EAP and LAP. The "worst-case scenario" yielded a Se and Sp of 58% and 51%, respectively, at EAP and 84% and 70%, respectively, at LAP.

Conclusion On CBCT, EAP showed limited accuracy. LAP provided the best tumor detectability.

Key Points

- *The early arterial phase (EAP) yielded poor accuracy: Se = 58% and Sp = 51% ($p < 0.0001$).*
- *The late arterial phase (LAP) phase yielded good accuracy: Se = 84% and Se = 70% ($p = 0.02$).*
- *The probability of a correct diagnosis at the EAP was 60%.*

Keywords Chemoembolization, therapeutic · Liver neoplasms · Cone beam computed tomography · Multidetector computed tomography · Data accuracy

✉ Olivier Pellerin
Olivier.pellerin@aphp.fr

[1] INSERM U970, Paris, France

[2] Université Paris Descartes, Sorbonne Paris Cité, Paris, France

[3] Department of Interventional Radiology, Hôpital Européen Georges Pompidou, Assistance Publique - Hôpitaux de Paris, 20 rue Leblanc, 75015 Paris, France

[4] Clinical Research Unit, Hôpital Européen Georges Pompidou, Assistance Publique - Hôpitaux de Paris, Paris, France

[5] INSERM U1418, Paris, France

[6] Department of Digestive Oncology, Hôpital Européen Georges Pompidou, Assistance Publique - Hôpitaux de Paris, Paris, France

Abbreviations

CBCT	C-arm cone beam computed tomography
CI	Confidence interval
CRCLM	Colorectal cancer liver metastases
EAP	Early arterial phase
ICC	Intra-class correlation coefficient
LAP	Late arterial phase
LR	Likelihood ratio
MDCT	Multidetector computed tomography
Se	Sensitivity
Sp	Specificity

Introduction

C-arm cone beam computed tomography (CBCT) is a valuable adjunct to conventional angiography. It provides useful cross-sectional imaging for patients undergoing intra-arterial liver treatment [1, 2]. Dual-phase CBCT imaging consists of two successive rotations of the C-arm, allowing the study of liver enhancement at two sequential times (early arterial phase (EAP) and late arterial phase (LAP)) of the same hepatic level during hepatic arterial injection. Dual-phase CBCT was recommended to increase hepatocellular carcinoma (HCC) detection during TACE procedures [3]. The accuracy of dual-phase CBCT for the detection of HCC is similar to that of MDCT [4]. Moreover, this approach is an accurate method to predict tumor response after TACE [5].

Colorectal cancer liver metastases (CRCLM) are increasingly treated by various intra-arterial approaches, such as irinotecan eluting beads chemoembolization (DEBIRI), hepatic intra-arterial chemotherapy, and radioembolization [6]. The delivery of the therapeutic compound in CRCLM is performed in a lobar manner and differs from HCC chemoembolization, which requires super-selective chemoembolization [7–9]. The microcatheter position in the hepatic arterial network needs to be adequately determined to reach all downstream vascularized tumors. Thus, these approaches require clear identification of tumor location, size, and boundaries. However, CRCLM do not have the same angiographic pattern as HCCs. Their angiographic visibility is limited (detection rate is 16.3%) and CRCLM detection can be improved by dual-phase (detection rate of 46% at the EAP and 95.3% at the LAP) [10]. However previous studies did not address sensitivity (Se) and specificity (Sp) of dual-phase CBCT as compared with MDCT. Therefore, we conducted this study in order to investigate the accuracy of dual-phase CBCT for the detection of CRCLM compared with MDCT in patients undergoing intra-arterial treatment.

Material and methods

Patient study selection

This is a single-center observational study that ran from March 2014 to December 2016. All consecutive patients with CRCLM referred for intra-arterial hepatic treatment (DEBIRI, TARE, hepatic intra-arterial chemotherapy) were screened at the liver tumor conference for intra-arterial therapy. The local ethics committee approved the study and all patients provided informed consent before inclusion.

MDCT

Baseline MDCT was performed within the 15 days before intra-arterial therapy with a Siemens Somatom Definition AS^{+} 128-slice CT unit (Siemens Healthineers). Acquisition parameters are summarized in Table 1.

Dual-phase CBCT

Images were acquired using a flat-panel angiographic system (Artis Zee; Siemens Healthineers). Dual-phase CBCT is a sequential acquisition of two, back-to-back CBCT scans, EAP and LAP using only one intra-arterial injection of iodine, as described by Lin et al [3]. The two scans were triggered at 3 s (EAP) and 18 s (LAP) after a selective single injection of pure contrast medium (15 mL iobitridol 350 with 25 mL saline flush power injected) through a 2.7-Fr coaxial microcatheter (Progreat®; Terumo) placed into the proper hepatic artery. Patients were instructed before the procedure to hold their breath for 21 s (single breath hold) during the two consecutive spins to avoid motion artifacts. Acquisition parameters and injection parameters are summarized in Table 1.

Image analysis

The portal phases of MDCT images and the two phases of CBCT (EAP and LAP) were retrieved from the PACS and anonymized. The MDCT arterial phase was set up to map the liver arterial network to facilitate navigation and was not used for the accuracy study. Two experienced readers in diagnostic and interventional radiology (10 years of practice) independently interpreted the images on a Syngo workstation (Siemens Healthineers). The readers were blinded to the number and location of liver CRCLM, and image analysis consisted of three successive steps.

First step, each reader, independently, evaluated the MDCT images and recorded the number, location, and maximum diameter (at the portal phase) of each hepatic lesion, segment by segment, on the MDCT portal phase (Couinaud segmentation) [11] and classified each lesion in three categories: (a) certainly a CRCLM: spheroid lesion with the following characteristics: hypodensity relative to normal liver parenchyma on unenhanced CT, hypodense on hepatic arterial phase CT with a thin hyper enhanced corona, and a bull's eye appearance at the portal venous phase (central hypodensity surrounded by thick enhanced corona) [12]; (b) certainly not a CRCLM: simple cyst, benign liver tumor, other; (c) undetermined lesion: inability to characterize the lesion.

Second step, a week later, each reader examined the dual-phase CBCT images in a random and different order

Table 1 Image modality acquisition parameters

	MDCT	C-arm CBCT
System	Siemens Somatom Definition AS$^+$ 128-slice Siemens Healthcare	Artis Zee; Siemens Healthcare
Acquisitions parameters	Scan time: 0.7 s Field of view: 40 × 60 Scan length: 480 mm Rotation time: 0.5 s Slice thickness: 0.6 mm Slice reconstruction thickness: 3 mm Collimation: 128 × 0.6 mm Matrix: 512 × 512	C-arm rotation: 220° clockwise arc. 312 projection images (30 frames/s) Scan time: 5 s Field of view = 30 × 40 cm Reconstruction algorithm: Feldkamp back Voxel size: 0.5 mm^3 isotropic Slice thickness = 1 mm Slice reconstruction thickness = 3 mm Matrix 512 × 512
Tube settings	Kv: 120 Effective mAs: 170	Kv: 90 Effective mA: 300
Acquisitions protocol	Tri-phasic: Unenhanced Arterial phase triggered at 20 s Portal phase triggered at 70 s	Dual-phase: Early arterial phase triggered at 3 s Late arterial phase triggered at 18 s
Injection protocol	Q = 3 mL/s V = 100 ml iobitridol PSI = 300 Injection site: Antecubital vein	Q = 4 mL/s V = 40 mL (15 mL iobitridol 350 + 25 mL saline flush) PSI = 300 Injection site: proper hepatic artery
Power injector used	Medrad® Stellan® Bayer HealthCare	Medrad® Mark 7 Arterion® Bayer HealthCare
Contrast media used	Iobitridol, 350 mg I/mL, Guerbet	Iobitridol, 350 mg I/mL, Guerbet

Q, injection flow rate; *V*, volume of injection; *PSI*, pound per square inch; *CBCT*, C-arm cone beam computed tomography; *MDCT*, multidetector computed tomography

than that used for the MDCT images, in order to avoid learning bias. They classified each lesion in three similar categories: (a) certainly a CRCLM: round and delineated hypodense areas surrounded by hyperdense capillaries at the EAP together with thin enhanced septa surrounded by a thick rim enhancement at the late arterial phase (Fig. 1); (b) certainly not a CRCLM: simple cyst, benign liver tumor, other etc; (c) undetermined lesion: inability to characterize the lesion.

Third step, after completing the reading of the dual-phase CBCT images, each reader analyzed the reasons why lesions were missed by dual-phase CBCT and classified them into one only of the three categories: (a) liver truncation, (b) streak artifacts, (c) the absence of tumor enhancement (Fig. 2). To validate the visual perception of the readers, both calculated the tumor-to-liver contrast ratio for both phases as described by Bechara et al by drawing a region of interest in a normal part of the liver and in three representative lesions on both phases [13].

Statistical analysis

Tumor size was measured in MDCT portal phases and both CBCT phases: The inter-observer agreement of tumor size was assessed using intra-class correlation coefficients (ICC) as described by Shrout and Fleiss [14]. ICC values were classified into four categories: ICC < 0.40, poor agreement; ICC from 0.40 to 0.60, moderate agreement; ICC from 0.60 to 0.80, substantial agreement; and ICC > 0.80, good agreement [14]. The reliability of the tumor size measurements on dual-phase CBCT, compared with that measured by MDCT, was evaluated using the Bland–Altman method [15]. The kappa coefficient was calculated for estimating inter-reader agreement between the two readers.

The diagnostic accuracy for colorectal cancer liver metastases (Se, Sp, likelihood ratios (LR), and predictive values) of dual-phase CBCT was assessed according to two different methods of analysis, as described by Simel et al [16]:

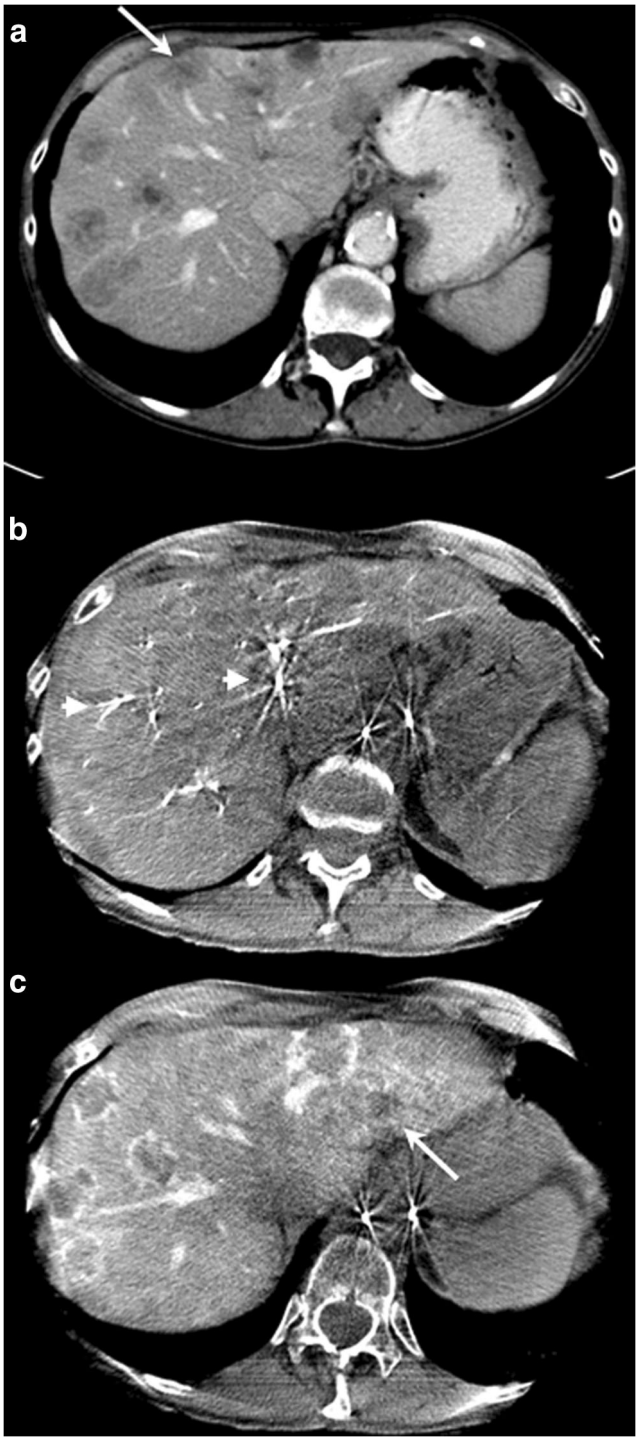

Fig. 1 MDCT at the portal phase (3-mm thickness) (**a**). Dual-phase C-arm CBCT (3-mm thickness): EAP (**b**) and LAP (**c**) for a 53-year-old woman with widespread liver invasion by CRCLM. Panel **a** shows six tumors involving segments II, III, IV, V, and VI appearing as hypodense lesions surrounded by liver enhanced parenchyma. The EAP (**b**) shows three tumors with moderate peripheral enhancement associated with a minimal streak artifact from catheter or contrast media (white arrow head). All three lesions were classified as uncertain by readers. The LAP (**c**) shows five lesions with a peripheral corona surrounding the tumor classified as certainly CRCLM. Readers classified the segment II lesion as uncertain (white arrow). The lesion in segment IV was missed by the both phases (**a**, white arrow)

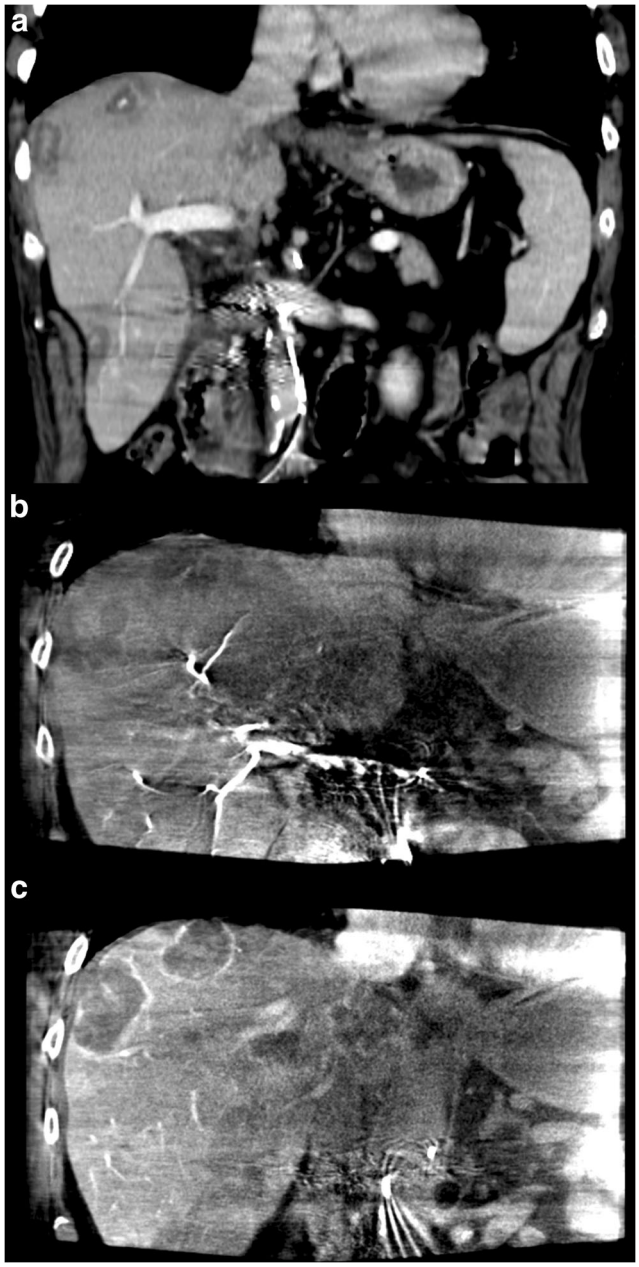

Fig. 2 MDCT at the portal phase (3-mm thickness) (**a**). Dual-phase C-arm CBCT (3-mm thickness): EAP (**b**) and IAP (**c**) for a 64-year-old man with widespread liver invasion by CRCLM. Panel **a** shows a coronal view of four tumors involving segments IV, V, and VIII. Due to the limitation of the field of view in the *Z*-axis, segments V and VI are truncated at both phases (EAP (**b**) and LAP (**c**) in a coronal view) and lesion is not visible

– First, calculations were done using a six-cell matrix including uninterpretable observations. In this case, only patients with positive or negative results are considered in the calculation of the sensitivity and specificity. The sensitivity and specificity are therefore conditional probabilities (e.g., conditional to an interpretable test result). In this case, we also provide the yields of CBCT results

(e.g., the ability of CBCT to give a decisional result) for a positive or negative MDCT test.
– Second, a conservative approach ("worst-case scenario") where uncertain results of the dual-phase CBCT readings, regardless of the reason (e.g., missed lesion because of streak artifacts, the absence of tumor enhancement, or liver truncation), were forced to either the group of dual-phase CBCT—certainly not a CRCLM in the case of MDCT—certainly a CRCLM or to the group of dual-phase CBCT—certainly a CRCLM in the case of MDCT—certainly not a CRCLM.

The 95% confidence intervals (CI) of proportions were calculated using the Wilson method and the CI of LR were calculated using the log method [17]. We compared the Se and Sp of the two phases using McNemar's test. A p value of 0.05 was considered to indicate statistical significance. Statistical analysis was performed with SAS software version 9.4 (SAS Institute).

Results

Patient demographic data

Between March 2014 and December 2016, 103 consecutive patients were screened. Fifty patients were excluded: 36 had a delay between MDCT and intra-arterial treatment > 15 days and 14 had an inappropriate MDCT technique (slice thickness > 3 mm). Dual-phase CBCT failed in four patients and they were excluded from the study. In total, dual-phase CBCT was successfully performed in 49 included patients who were analyzed. Twenty-four (49%) patients were assigned to DEBIRI and 25 (51%) to hepatic intra-hepatic chemotherapy. Biotherapies were stopped 30 days before the intra-arterial procedure. The flow diagram of the study participants and the patient baseline characteristics are shown in Fig. 3 and Table 2, respectively.

Tumor diagnosis and measurement

Both readers identified a total of 307 hepatic lesions (8 ± 4 [3–16] lesions/patient) on the MDCT portal phase with a mean maximum diameter of 32 ± 16 mm (Table 3). On CBCT images, reader 1 identified 240 lesions at the LAP (36 mm ± 16 [12–98]) and 277 at the LAP (33 mm ± 15 [12–97]). On CBCT images, reader 2 identified 246 lesions at the EAP (37 mm ± 16 [11–99]) and 281 at the LAP (34 mm ± 16 [11–98]). Reader 1 missed 49 lesions at the EAP because of streak artifacts ($n = 12$) or the absence of enhancement ($n = 37$). At the LAP, reader 1 missed 12 lesions because of the absence of enhancement. Reader 2 missed 43 lesions at the EAP because of streak artifacts ($n = 10$) or the absence of enhancement ($n = 33$). At the LAP, reader 2 missed eight lesions because of the absence of enhancement. In addition, liver segment truncation was responsible for a total of 18 missed lesions in nine (18%) patients for both readers (single liver segment truncation in four patients, three segment truncations in five patients). The mean tumor-to-liver contrast ratio was 0.45 at the EAP and 1.85 at the LAP ($p < 0.001$).

Inter-reader agreement for tumor size estimation

The tumor size evaluated by both readers for the different image modalities was inter-correlated ($p < 0.001$). The intra-class correlation coefficient (ICC) was excellent (> 0.74) as the ICC between 0.949 and 0.992 for all measurements.

Inter-modality agreement for tumor size estimation

The Bland–Altman plots showed good agreement between dual-phase CBCT and MDCT for both readers. Figure 4 shows the Bland and Altman plot comparing MDCT with the two phases of the dual-phase CBCT for each reader. For both readers, a significant ($p = 0.003$) mean diameter measurement overestimation of 1.9 mm and 2.02 mm was calculated at the EAP and LAP, respectively, when compared with MDCT with a very small proportion of variance (0.21 and 0.19 for each phase, respectively) for both readers.

Diagnostic accuracy of tumor nature using dual-phase CBCT

Among the 307 lesions detected by MDCT, 264 (86%) were classified by both readers as certainly CRCLM. Comparisons of results obtained by both readers are depicted in Table 3. Forty-three (14%) were classified as certainly not CRCLM (simple cyst $n = 39$, adenoma $n = 3$, angioma $n = 1$). Reader 1 classified 157 (51%) lesions at the EAP as certainly CRCLM and 226 (74%) at the LAP. Reader 2 classified 156 (51%) lesions at the EAP as certainly CRCLM and 231 (75%) at the LAP.

The accuracy was calculated with the results of reader 1 only, because the kappa test ($\kappa = 0.84$) showed good concordance between the two readers. The EAP yielded a Se of 93% and a Sp of 85% and the LAP a Se of 99% and a Sp of 88% using the six-cell matrix accuracy method (Table 4). The positive likelihood (LR+) ratios, reflecting the odds of a positive test in favor of disease, were 6 and 9 for the EAP and LAP, respectively. Thus, there was a six- and ninefold greater chance to correctly identify CRCLM with dual-phase CBCT when CRCLM was diagnosed by MDCT. In other words, the

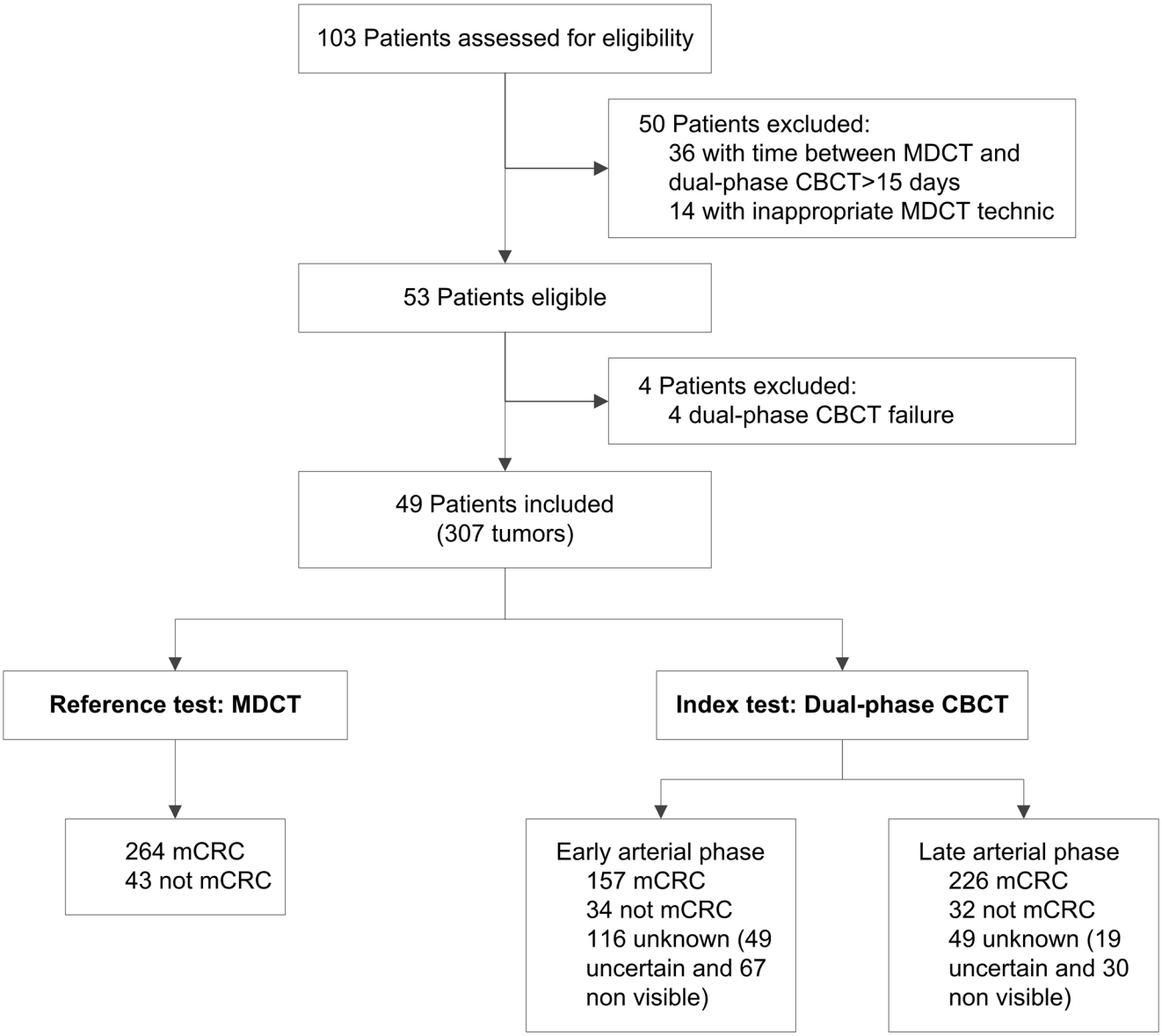

Fig. 3 Flow diagram of the study participants

probability to correctly diagnose a CRCLM at the EAP and the LAP was 60% and 90%, respectively (Table 5). The low value of the likelihood ratio and the high value of Se and Sp especially at the AEP indicate an overestimation of the Se and Sp mainly due to the high number of uncertain results (Table 4).

When assessing the "worst-case scenario," we calculated a Se of 58% and a Sp of 51% at the EAP ($p < 0.0001$) and 84% Se and 70% Se at the LAP ($p = 0.02$) (Table 5).

Discussion

The first result is the low yield (i.e., the probability to give a decisional result) of EAP compared with LAP for both "MDCT—certainly CRCLM" and "MDCT—certainly not CRCLM." This explains the discrepancies between our two methods of performance analysis for the two CBCT arterial phases. When using the six-cell matrix, both phases of the CBCT gave very good Se and Sp, negative LR, and good positive LR. In the "worst-case analysis" (when considering the non-diagnostic results), we observed a significant decrease of diagnostic performance of both phases, much stronger for EAP than for LAP CBCT.

The two statistical approaches gave different Se and Sp. The six-cell matrix allows the calculation of Se and Sp while some results are uncertain. In other words, Se and Sp should be labeled as conditional Se and conditional Sp since they both do not take into account the proportion of uncertain results. The greatest the proportion of

Table 2 Patient baseline characteristics

Baseline characteristics	Value
Demographics	
No. of patients	49
Age (years)	63 ± 15 [41–81]
Body mass index	24 ± 4 [19–34]
Sex (male/female)	23/26
ECOG performance status (0/1)	27/22
Child-Pugh class (A/B)	45/4
% of tumor involvement into the liver < 25%, > 26%–< 50%, > 51%	12/32/5
No. of hepatic lesion per patient (on MDCT)	8 ± 4 [3–16]
Hepatic lesion size (mm)	31 ± 16 [10–98]
Previous chemotherapy regimens	
Oxaliplatin-based	49 (100%)
Irinotecan-based	32 (65%)
Biotherapies	18 (37%)
Serum tests	
Basal ACE (μg/mL)	171 ± 147[2–510]
Basal CA 19.9. (Ku/L)	1689 ± 866 [14–2732]
kRAS status (wild/mutant)	35/10
Albumin (g/dL)	34 ± 4.6 [25–45]
Total bilirubin (μmol/L)	12 ± 5 [4–20]
AST (UI/L)	130 ± 45 [28–133]
ALT (UI/L)	75 ± 44 [31–120]
Alkaline phosphatase (UI/L)	238 ± 58 [88–449]
GGT (UI/L)	49 ± 21 [1–118]
INR	1.2 ± 21 [23–118]
Intra-arterial treatment	49
DEBIRI*	24
Intra-arterial chemotherapy	25

*DBIRI was performed with Irinotecan DC-Bead loaded bead (BTG International). Data are mean ± SD [range] or *n* (%). *MDCT*, multidetector computed tomography; *SD*, standard deviation

uncertain results, the greatest the difference between estimates of Se and Sp with the six-cell matrix and the worst-case scenario. The true value of Se and Sp probably lies between these two estimates. Meanwhile, if the method cannot improve, only LAP of CBCT should be used for clinical purpose.

However, these two methods have advantages and are of interest. The six-cell matrix allows the calculation of Se and Sp while some results are uncertain. In such condition, when using a four-cell matrix (worst-case scenario), uncertain results needs to be dispatched to false negative and false positive. This leads to inaccurate Se and Sp. In our study, two categories of "uncertain results" were coexisting: uncertain diagnostic: accounting for a visible lesion without possibility to allocate to a diagnostic (49 (16%) and 19 (6%) cases at the EAP and LAP respectively), and missing lesions (a lesion that was not seen because of liver truncation, streak artifact…) that occur in 67 (22%) and 30 (10%) cases at the EAP and LAP respectively. On the one hand, when using the six-cell matrix, uncertain diagnostic and missing lesions were pooled, artificially inflating the number of uncertain diagnostic and yielding a better Sp and Se. On the other hand, with the four-cell matrix, the false negative and false positives are expended and yield a low Se and Sp. In other words, Se and Sp calculated with the six-cell matrix express the intrinsic Se and Sp of visible lesions and the Se and Sp from the four-cell matrix give "real-life" situation. But Se and Sp are potentially underestimated.

These results are consistent with Schernthaner et al. In a study evaluating the tumor detection rate by dual-phase CBCT (MRI as reference) using the same imaging protocol, they reported a detection rate of 46% at the EAP and 95.3% at the LAP [10]. However, our study provides more insight into the accuracy question. Schernthaner et al attempted to address this question, focusing on lesion

Table 3 Image modalities, lesion measurement, and diagnostic

	MDCT	Dual-phase CBCT early arterial phase	Dual-phase CBCT late arterial phase
Reader 1			
Number of lesions seen	307	240 (78%)	277 (91%)
Lesion diameters	32 mm ± 16 [10–98]	36 mm ± 16 [12–98]	33 mm ± 15 [12–97]
Lesion type			
Certainly CRCLM	264 (86%)	157 (51%)	226 (74%)
Certainly not CRCLM*	43 (14%)	34 (11%)	32 (10%)
Undetermined	NA	49 (16%)	19 (6%)
Tumor-to-liver contrast ratio	NA	0.45	1.85
Missed lesion by dual-phase CBCT	NA	67 (22%)	30 (10%)
Causes of lesions missed			
Streak artifacts	NA	12 (4%)	0
Absence of enhancement	NA	37 (12%)	12 (4%)
Liver truncation	NA	18 (6%)	18 (6%)
Reader 2			
Number of lesions seen	307	246 (80%)	281 (92%)
Lesion diameter	32 mm ± 16 [11–99]	37 mm ± 16 [11–99]	34 mm ± 16 [11–98]
Lesion type			
Certainly CRCLM	264 (86%)	156 (51%)	231 (75%)
Certainly not CRCLM*	43 (14%)	26 (8%)	36 (12%)
Undetermined	NA	64 (21%)	14 (5%)
Tumor-to-liver contrast ratio	NA	0.45	1.85
Missed lesion by dual-phase CBCT	NA	61 (20%)	26 (8%)
Causes of lesions missed			
Streak artifacts	NA	10 (3%)	0
Absence of enhancement	NA	33 (11%)	8 (2%)
Liver truncation	NA	18 (6%)	18 (6%)

*Simple cyst, adenoma, or angioma. Data are mean ± SD [range] or *n* (%). *CRCLM*, colorectal cancer liver metastases; *CBCT*, C-arm cone beam computed tomography; *MDCT*, multidetector computed tomography; *SD*, standard deviation

detection rate but not on accuracy of CRCLM diagnosis [10]. Therefore, the goal of their study was to report the detectability rate of a lesion with the assumption that all liver lesions were CRCLM. In contrast, herein, we took into account the real nature of the liver lesion and provided more realistic ("real-life") Se and Sp. We also took into account the two possible scenarios (six-cell matrix and "worst-case scenario") to describe the possible pitfall of dual-phase CBCT in a global approach.

Otherwise, our results confirm that dual-phase CBCT yields good inter-reader and inter-modality correlations regarding size and number of lesions as previously described [18].

The clinical relevance of using dual-phase CBCT to diagnose and size tumors should be weighted against the fact that intra-arterial treatment of CRCLM is overwhelmingly administered in a lobar approach, and it is not recommended to perform selective catheterization of tumor feeders [8]. Indeed, CRCLM arterial feeders are particularly small relative to those of HCC or NETs, and their angiographic visibility is poor [10]. CRCLM are often more diffuse and numerous than depicted on imaging, explaining the high recurrence rate after liver resection (60% at 2 years) and the recommendation to deliver intra-arterial therapy treatment in a lobar manner rather than selective [7].

The accuracy of dual-phase CBCT has been extensively studied using protocols dedicated to HCC imaging. The absence of a dedicated, widely accepted acquisition protocol for CRCLM highlights two main limitations.

First, pure contrast medium injection induces a high frequency of streak artifacts masking adjacent metastases. This was borne out by the low tumor-to-liver contrast ratio at the EAP (0.45). Indeed, we observed more streak artifacts at the EAP than at the LAP (4% vs 0%) and the tumor-to-liver enhancement ratio was in some cases too poor to delineate the tumor (12% vs 4% for the LAP). Conversely, in the case of HCC, EAP is almost as accurate as LAP (Se = 72% vs Se =

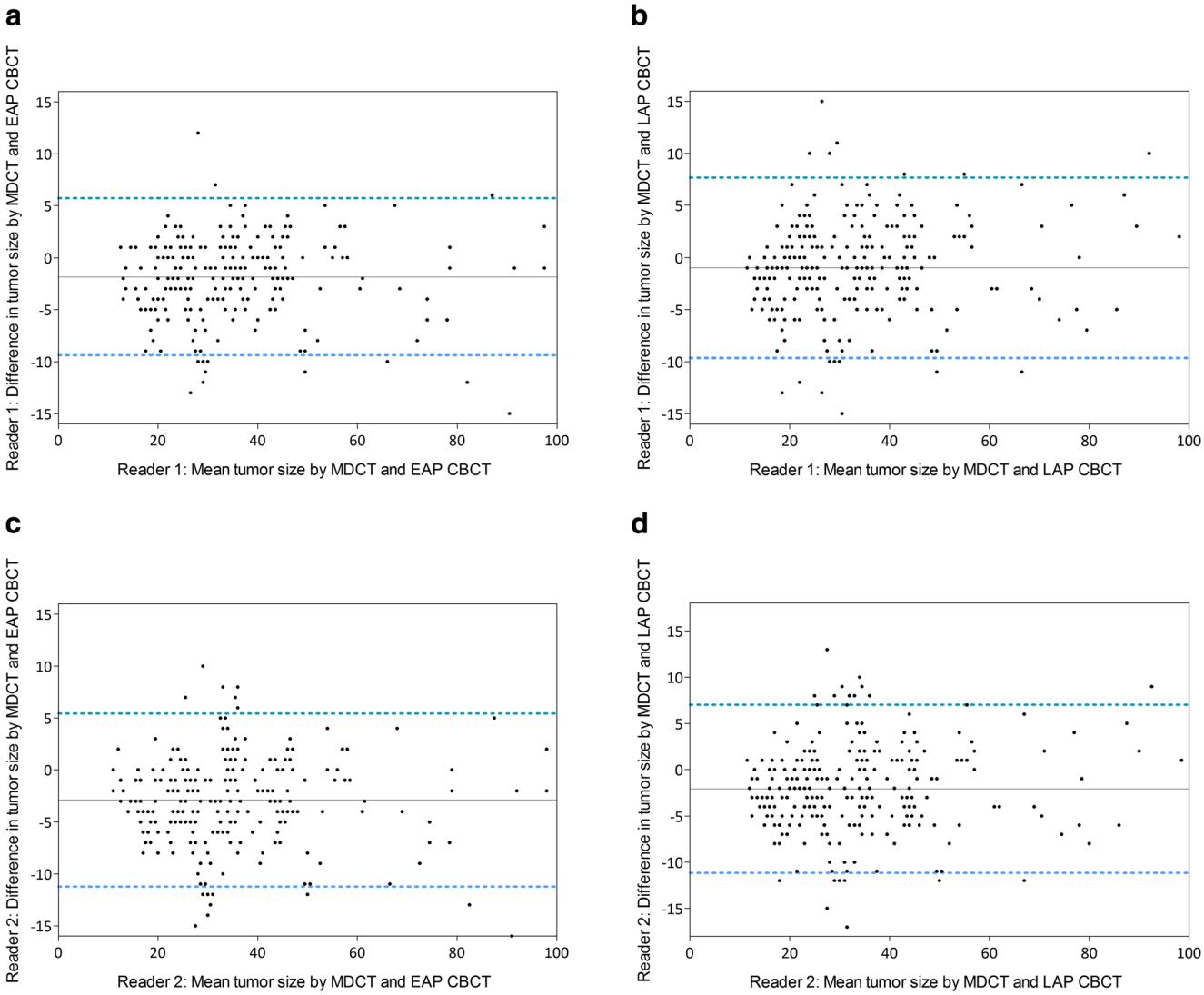

Fig. 4 Bland and Altman plots. The *Y*-axis shows the difference between the 2 paired measurements (MDCT and early arterial phase CBCT (EAP CBCT), panel **a** and **c**, and MDCT and late arterial phase CBCT (LAP CBCT), panels **b** and **d**) and the *X*-axis the average of these 2 measurements. The plain line represents the mean value of the difference and the dashed lines are the limits of agreement (± 1.96 SD). The Bland and Altman analysis shows a good agreement between the dual-phase CBCT and MDCT for both readers with a minimal degree of variance of tumor measurement. Dual-phase C-arm CBCT tends to overestimate the tumor diameter, by 1.9 mm and 2.02 ($p = 0.003$) at the EAP and LAP respectively with a very small proportion of variance (0.21 and 0.19 for each phase, respectively) for both readers when compare with MDCT

87%) [4, 19], as tumor enhancement led to only 13% undiagnosed tumors in spite of streak artifacts [19]. The use of diluted contrast media has been proposed by Lucatelli et al [20]. This would reduce beam-hardening artifacts at the cost of a decrease of CRCLM arterial enhancement.

Second, a more relevant timing of acquisition after injection might improve detectability. Indeed, we found that 22% and 10% of the lesion were not visible at the EAP and the LAP respectively. Shady et al reported similar findings in a study that evaluated the enhancement patterns of CRCLM with hepatic MDCT arteriography [21]. The CT acquisitions were triggered 4 s after intra-arterial injection of the contrast media. They reported that 60% of CRCLM were fully enhanced, 24% were partially enhanced, and 16% were non-enhanced. There are two possible explanations for these findings. First, CRCLM have a different pattern of vascularization, as they are supplied by both the hepatic artery and the portal vein at variable ratios [22, 23]. Second, the phenomenon known as "late enhancement" corresponds to late and progressive accumulation of contrast agent in the interstitial spaces contained within the fibrosis, which could explain the 67% of CRCLM not visible at the EAP which became visible at the LAP [24]. Based on these facts, a longer delay after contrast injection, before scanning, would probably increase the accuracy of the dual-phase CBCT.

Table 4 Six-cell matrix table of diagnostic result per image modality

		MDCT		Total
		Certainly CRCLM	Certainly not CRCLM	
Dual-phase CBCT early arterial phase	Certainly CRCLM	153	*4*	157
	Undetermined	*99*	*17*	116
	Certainly not CRCLM	*12*	22	34
	Total	264	43	307
Dual-phase CBCT late arterial phase	Certainly CRCLM	222	*4*	226
	Undetermined	*40*	*9*	49
	Certainly not CRCLM	*2*	30	32
	Total	264	43	307

Cells in italics are summed for the calculations of the worst-case scenario (see Table 5). *CRCLM*, colorectal cancer liver metastases; *CBCT*, C-arm cone beam computed tomography; *MDCT*, multidetector computed tomography

Another important limiting factor is the significant intrinsic limitation of 30/40 flat-panel detectors, resulting in the incapacity to cover the whole liver volume in some cases. Indeed, 18 (6%) lesions were missed in truncated liver segments. This limitation was even more apparent when applying the "worst-case scenario," highlighting the impact of truncated segments on accuracy. This specific flaw of CBCT is well recognized but not considered in the accuracy calculation [4, 19, 25]. Manufacturers have developed specific applications based on double spin with a table shift in the *X*-axis to enlarge the field of view [26]. Our study found the truncated liver segments to be segments VIII, V, and VI. A table shift on the *Z*-axis would have been the better option to overcome this limitation. Moreover, this application would compromise the dual-phase acquisition and expose patients to two supplementary acquisitions, due to the time required for rotation, resulting in increased radiation and contrast medium exposure. Finally, this application is not commercially available. Larger flat-panel detectors could of course overcome, at least in part, this limitation.

As a last limitation, the dual-phase CBCT accuracy was evaluated with MDCT as the gold standard. It is known that MDCT had a lower accuracy than MRI especially in chemotherapy-treated patient. Thus, it is possible that the accuracy of dual-phase CBCT would be much lower when compared with MRI as a gold standard.

These findings suggest that it is not possible to rely on the EAP alone during intra-arterial liver treatment to correctly diagnose a tumor, despite good inter-reader correlation and a good correlation in tumor sizing. There is an unacceptable risk of 37% of not being able to distinguish between CRCLM and other types of lesions. There is also a risk of underestimating the number of CRCLM. Only the LAP yielded good tumor detectability, allowing for safe intra-arterial hepatic treatment.

Table 5 Accuracy of dual-phase C-arm CBCT

	6-cell matrix		Worst-case scenario		
	Early arterial phase	Late arterial phase	Early arterial phase	Late arterial phase	*p*
Sensitivity (%)	93 [88–96]	99 [97–99]	58 [59–64]	84 [79–3]	< 0.0001
Specificity (%)	85 [67–94]	88 [73–95]	51 [37–65]	70 [55–81]	0.0215
Positive predictive value (%)	97 [94–99]	98 [95–99]	88 [82–92]	94 [91–97]	
Negative predictive value (%)	65 [48–78]	94 [80–98]	17 [11–24]	42 [31–53]	
LR+	6 [2–16]	9 [4–23]	1 [0.8–1.6]	3 [1.7–4.4]	
LR-	0.09 [0.05, 0.17]	0.01 [0.00, 0.04]	0.8 [0.6–1.1]	0.2 [0.2–0.3]	
YD+	0.63	0.85	NA	NA	
YD-	0.60	0.79	NA	NA	

Value corresponds to McNemar's test comparing sensitivities and specificities of the early and the late arterial phases. LR+ is the conditional likelihood ratio of a positive test, the odds of a positive test in favor of disease. LR- is the conditional likelihood ratio of a negative test; the odds of a negative test in favor of disease. YD+ is the probability of a positive or a negative result when disease is present. YD- is the probability of a positive or a negative result when disease is absent

Funding The authors state that this work has not received any funding.

Compliance with ethical standards

Guarantor The scientific guarantor of this publication is Olivier Pellerin, Deputy Head of the interventional radiology department at Hôpital Européen Georges Pompidou.

Conflict of interest The authors of this manuscript declare no relationships with any companies, whose products or services may be related to the subject matter of the article.

Statistics and biometry Hélena Pereira, PhD, one of the authors, has significant statistical expertise.

Informed consent Written informed consent was obtained from all subjects (patients) in this study.

Ethical approval Institutional Review Board approval was obtained.

Methodology
- prospective
- observational
- performed at one institution

References

1. Meyer BC, Frericks BB, Voges M et al (2008) Visualization of hypervascular liver lesions during TACE: comparison of angiographic C-arm CT and MDCT. AJR Am J Roentgenol 190: W263–W269
2. Miyayama S, Matsui O, Yamashiro M et al (2009) Detection of hepatocellular carcinoma by CT during arterial portography using a cone-beam CT technology: comparison with conventional CTAP. Abdom Imaging 34:502–506
3. Lin M, Loffroy R, Noordhoek N et al (2010) Evaluating tumors in transcatheter arterial chemoembolization (TACE) using dual-phase cone-beam CT. Minim Invasive Ther Allied Technol. https://doi.org/10.3109/13645706.2010.536243
4. Higashihara H, Osuga K, Onishi H et al (2012) Diagnostic accuracy of C-arm CT during selective transcatheter angiography for hepatocellular carcinoma: comparison with intravenous contrast-enhanced, biphasic, dynamic MDCT. Eur Radiol 22:872–879
5. Loffroy R, Lin M, Yenokyan G et al (2013) Intraprocedural C-arm dual-phase cone-beam CT: can it be used to predict short-term response to TACE with drug-eluting beads in patients with hepatocellular carcinoma? Radiology 266:636–648
6. de Baere T, Deschamps F (2011) Arterial therapies of colorectal cancer metastases to the liver. Abdom Imaging 36:661–670
7. Lencioni R, Aliberti C, de Baere T et al (2014) Transarterial treatment of colorectal cancer liver metastases with irinotecan-loaded drug-eluting beads: technical recommendations. J Vasc Interv Radiol 25:365–369
8. Deschamps F, Elias D, Goere D et al (2011) Intra-arterial hepatic chemotherapy: a comparison of percutaneous versus surgical implantation of port-catheters. Cardiovasc Intervent Radiol 34:973–979
9. Salem R, Lewandowski RJ, Gates VL et al (2011) Research reporting standards for radioembolization of hepatic malignancies. J Vasc Interv Radiol 22:265–278
10. Schernthaner RE, Haroun RR, Duran R et al (2016) Improved visibility of metastatic disease in the liver during intra-arterial therapy using delayed arterial phase cone-beam CT. Cardiovasc Intervent Radiol 39:1429–1437
11. Bismuth H (2013) Revisiting liver anatomy and terminology of hepatectomies. Ann Surg 257:383–386
12. Rosenthal MH, Kim KW, Fuchs CS, Meyerhardt JA, Ramaiya NH (2015) CT predictors of overall survival at initial diagnosis in patients with stage IV colorectal cancer. Abdom Imaging 40:1170–1176
13. Bechara B, McMahan CA, Moore WS, Noujeim M, Geha H, Teixeira FB (2012) Contrast-to-noise ratio difference in small field of view cone beam computed tomography machines. J Oral Sci 54: 227–232
14. Shrout PE, Fleiss JL (1979) Intraclass correlations: uses in assessing rater reliability. Psychol Bull 86:420–428
15. Bland JM, Altman DG (1986) Statistical methods for assessing agreement between two methods of clinical measurement. Lancet 1:307–310
16. Simel DL, Feussner JR, DeLong ER, Matchar DB (1987) Intermediate, indeterminate, and uninterpretable diagnostic test results. Med Decis Making 7:107–114
17. Wilson EB (1927) Probable inference, the law of succession, and statistical inference. J Am Stat Assoc 22:209–212
18. Pellerin O, Lin M, Bhagat N, Ardon R, Mory B, Geschwind JF (2013) Comparison of semi-automatic volumetric VX2 hepatic tumor segmentation from cone beam CT and multi-detector CT with histology in rabbit models. Acad Radiol 20:115–121
19. Loffroy R, Lin M, Rao P et al (2012) Comparing the detectability of hepatocellular carcinoma by C-arm dual-phase cone-beam computed tomography during hepatic arteriography with conventional contrast-enhanced magnetic resonance imaging. Cardiovasc Intervent Radiol 35:97–104
20. Lucatelli P, Corona M, Argirò R et al (2015) Impact of 3D rotational angiography on liver embolization procedures: review of technique and applications. Cardiovasc Intervent Radiol 38:523–535
21. Shady W, Sotirchos V, Pandit-Taskar N et al (2015) Enhancement patterns of colorectal liver metastases on pre-SIRT mapping CT arteriography correlates with FDG-PET SUVmax metabolic response. J Vasc Interv Radiol 2:S189–S190
22. Lin G, Lunderquist A, Hägerstrand I, Boijsen E (1984) Postmortem examination of the blood supply and vascular pattern of small liver metastases in man. Surgery 96:517–526
23. Haugeberg G, Strohmeyer T, Lierse W, Böcker W (1988) The vascularization of liver metastases. Histological investigation of gelatine-injected liver specimens with special regard to the vascularization of micrometastases. J Cancer Res Clin Oncol 114:415–419
24. Cuenod CA, Fournier L, Balvay D, Guinebretière JM (2006) Tumor angiogenesis: pathophysiology and implications for contrast-enhanced MRI and CT assessment. Abdom Imaging 31:188–193
25. Schernthaner RE, Lin M, Duran R, Chapiro J, Wang Z, Geschwind JF (2015) Delayed-phase cone-beam CT improves detectability of intrahepatic cholangiocarcinoma during conventional transarterial chemoembolization. Cardiovasc Intervent Radiol 38:929–936
26. Schernthaner RE, Chapiro J, Sahu S et al (2015) Feasibility of a modified cone-beam CT rotation trajectory to improve liver periphery visualization during transarterial chemoembolization. Radiology 277:833–841